Supporting Information: Diffusion of Water and Carbon Dioxide and Mixtures Thereof in Mg-MOF-74

S. Bendt, Y. Dong, and F. J. Keil*

Hamburg University of Technology, Institute of Chemical Reaction Engineering, Eissendorfer Strasse 38, D-21073 Hamburg, Germany

E-mail: keil@tuhh.de

Referred figures and tables in the article

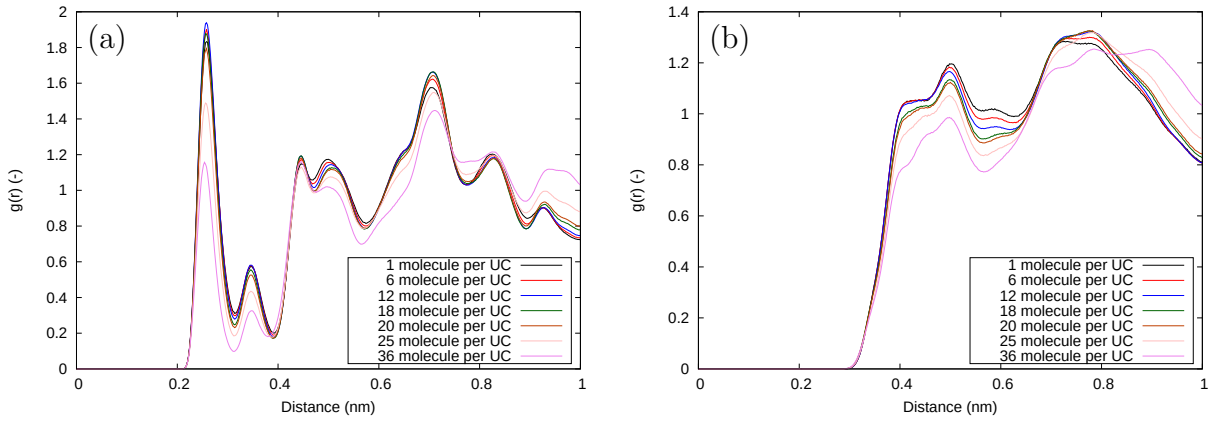

Figure S1: Pair distribution function for the carbon of the CO_2 molecule with respect to the Mg-atoms in the rigid (a) and in the flexible (b) framework. The results are based on the DFT-FF as described in the main article. The distance of 1 nm is approximately the mean distance form a Mg-ion to the channel center.

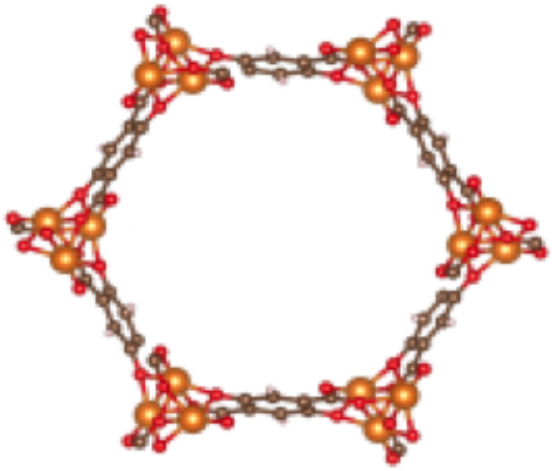

Figure S2: Unit cell of Mg-MOF-74. Magnesium is shown as orange, oxygen as red, carbon as brown and hydrogen as white.

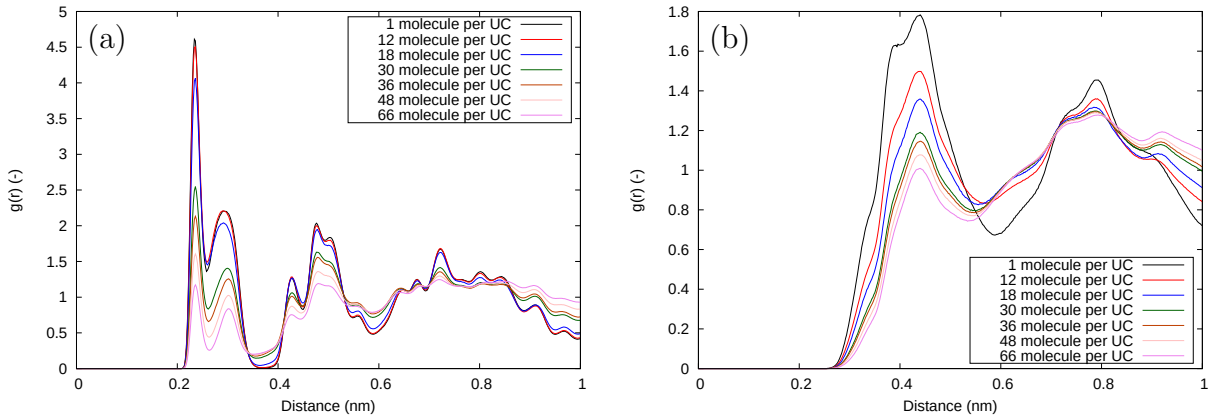

Figure S3: Pair distribution function for the oxygen of the water molecule with respect to the Mg-atoms in the rigid (a) and in the flexible (b) framework. The results are based on the DFT-FF as described in the main article. The distance of 1 nm is approximately the mean distance form a Mg-ion to the channel center.

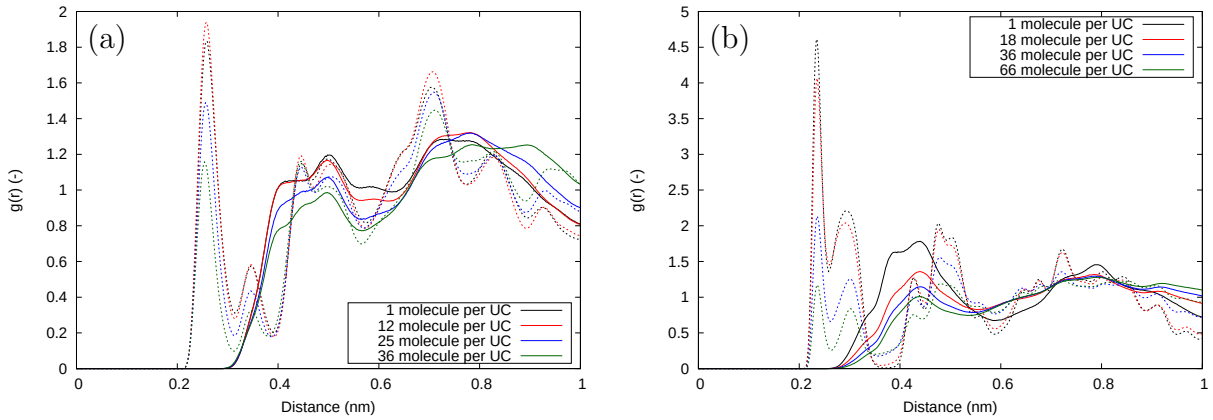

Figure S4: Comparison of the pair distribution function for the carbon of the CO_2 molecule (a) and the oxygen of the water molecule (b) with respect to the Mg-atoms in the framework. The dotted lines represent the results for the rigid case and the unbroken lines for the flexible one. The results are based on the DFT-FF as described in the main article. The distance of 1 nm is approximately the mean distance form a Mg-ion to the channel center.

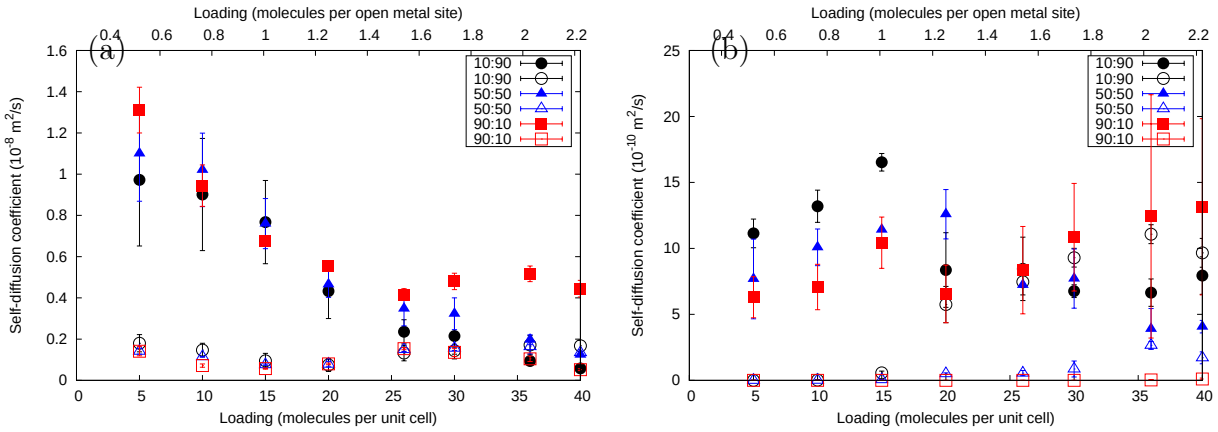

Figure S5: Self-diffusion coefficients for CO_2 (a) and H_2O (b) in three CO_2/H_2O-mixtures (90/10 (black dot), 50/50 (blue triangle), and 10/90 (red square)) as a function of total loading based on the DFT-FF in the rigid (open symbol) and in the flexible (closed symbols) framework. The lines represent the pure rigid (full line) and the flexible (dashed line) data, respectively.

Force field parameters

Table S1: Atomtypes used in the simulation with their corresponding point charges and Lennard-Jones parameters taken from the UFF,[S1] TIP3P(-Ew),[S2,S3] TIP5P,[S4,S5] TraPPE,[S6] and our previous work.[S7]

Atomtype	charge (elemental charge)	ϵ ($\frac{kJ}{mol}$)	σ (nm)	ϵ (K)	σ (Å)
Mg	1.558	0.464	0.269	55.857	2.691
Oa	-0.770	0.251	0.312	30.193	3.118
Ob	-0.880				
Oc	-0.907				
Ca	0.903	0.439	0.343	52.838	3.431
Cb	-0.313				
Cc	0.444				
Cd	-0.216				
Ha	0.182	0.184	0.257	22.142	2.571
H_H_2O (TIP3P)	0.417	0.000	0.000	0.000	0.000
O_H_2O (TIP3P)	-0.834	0.637	0.315	76.420	3.151
H_H_2O (TIP5P)	0.241	0.000	0.000	0.000	0.000
O_H_2O (TIP5P)	0.000	0.745	0.310	89.378	3.097
L_H_2O (TIP5P)	-0.241	0.000	0.000	0.000	0.000
O_CO_2	-0.700	0.656	0.305	79.000	3.050
C_CO_2	0.350	0.224	0.280	27.000	2.800

Table S2: Crossterm parameters for guest molecules based on the methodology refitted from previous study:[S7] Mixing parameters are refitted to Lennard-Jones functions.

Guest molecule atomtype	Framework atomtype	ϵ ($\frac{kJ}{mol}$)	σ (nm)	ϵ (K)	σ (Å)
H_H_2O	Mg	0.6605	0.239	79.444	2.390
	Oa	0.2295	0.263	27.605	2.626
	Ob				
	Oc				
	Ca	0.2172	0.273	26.126	2.734
	Cb				
	Cc				
	Cd				
	Ha	0.0001	0.602	0.011	6.018
O_H_2O	Mg	2.1587	0.244	259.630	2.442
	Oa	0.8380	0.315	100.792	3.145
	Ob				
	Oc				
	Ca	0.5169	0.340	62.171	3.401
	Cb				
	Cc				
	Cd				
	Ha	0.0000	0.100	0.000	1.000
O_CO_2	Mg	2.4069	0.234	289.479	2.343
	Oa	0.0378	0.387	4.459	3.874
	Ob				
	Oc				
	Ca	0.7499	0.327	90.190	3.269
	Cb				
	Cc				
	Cd				
	Ha	0.0001	0.100	0.000	1.000
C_CO_2	Mg	0.0001	0.594	0.0013	5.938
	Oa	1.3583	0.281	163.366	2.807
	Ob				
	Oc				
	Ca	0.3655	0.345	43.963	3.451
	Cb				
	Cc				
	Cd				
	Ha	0.0000	0.100	0.000	1.000

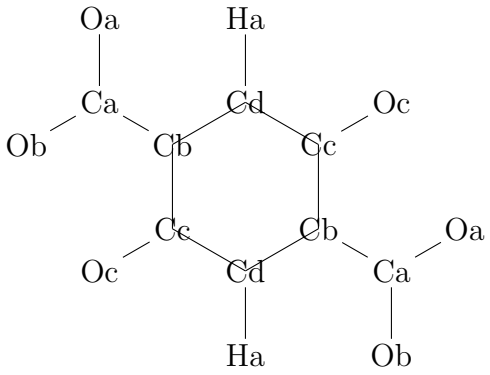

Figure S6: Description (schematically) of the atomtypes found in the organic linker of the framework.

Table S3: Interaction parameters for framework bonds based on the UFF.[S1]

i	j	r_0 (nm)	k_0 ($\frac{kJ}{mol \cdot nm^2}$)	$k_0^{reduced}$ ($\frac{kJ}{mol \cdot nm^2}$)
Mg	Oa	0.2035	135662.5	45220.8
Mg	Ob	0.2035		
Mg	Oc	0.2035		
Oa	Ca	0.1272	594414.3	198138.1
Ob	Ca	0.1272		
Oc	Cc	0.1343	505222.2	168407.4
Ca	Cb	0.1461	325952.2	108650.7
Cb	Cc	0.1379	387408.8	129136.3
Cb	Cd	0.1379		
Cc	Cd	0.1379		
Cd	Ha	0.1081	299306.3	99768.8

Table S4: Interaction parameters for framework angles based on the UFF.[S1]

i	j	k	k_θ ($\frac{kJ}{mol \cdot rad^2}$)	$k_\theta^{reduced}$ ($\frac{kJ}{mol \cdot rad^2}$)	θ_0 (deg)
Oa	Mg	Oa	8924.67	2974.89	109.47
Oa	Mg	Ob			
Oa	Mg	Oc			
Ob	Mg	Oc			
Oc	Mg	Oc			
Mg	Oa	Mg	1881.19	627.06	120
Mg	Oa	Ca	3501.58	1167.19	
Mg	Ob	Ca			
Mg	Oc	Mg	1881.19	627.06	
Mg	Oc	Cc	3334.18	1111.39	
Oa	Ca	Ob	12761.60	4253.87	
Oa	Ca	Cb	8501.23	2833.74	
Ob	Ca	Cb			
Ca	Cb	Cc	6327.47	2109.16	
Ca	Cb	Cd			
Cc	Cb	Cc	6914.26	2304.75	
Oc	Cc	Cb	8655.69	2885.23	
Oc	Cc	Cd			
Cb	Cc	Cd	6914.26	2304.75	
Cb	Cd	Cc			
Cb	Cd	Ha	3559.03	1186.34	
Cc	Cd	Ha			

Table S5: Interaction parameters for framework dihedrals based on the UFF. [S1]

i	j	k	l	k_ϕ ($\frac{kJ}{mol}$)	$k_\phi^{reduced}$ ($\frac{kJ}{mol}$)	ϕ (deg)	m (-)
Oa	Mg	Oa	Mg	0.00	0.00	180	2
Oa	Mg	Oa	Ca				
Ob	Mg	Oa	Mg				
Ob	Mg	Oa	Ca				
Oc	Mg	Oa	Mg				
Oc	Mg	Oa	Ca				
Oa	Mg	Ob	Ca				
Oc	Mg	Ob	Ca				
Oa	Mg	Oc	Mg				
Oa	Mg	Oc	Cc				
Ob	Mg	Oc	Mg				
Ob	Mg	Oc	Cc				
Oc	Mg	Oc	Mg				
Oc	Mg	Oc	Cc				
Mg	Oa	Ca	Ob	94.05	31.35		
Mg	Oa	Ca	Cb				
Mg	Ob	Ca	Oa	10.45	3.48		
Mg	Ob	Ca	Cb				
Mg	Oc	Cc	Cb	94.05	31.35		
Mg	Oc	Cc	Cd				
Oa	Ca	Cb	Cc	10.45	3.48		
Oa	Ca	Cb	Cd				
Ob	Ca	Cb	Cc				
Ob	Ca	Cb	Cd				
Ca	Cb	Cc	Oc	52.25	17.42		
Ca	Cb	Cc	Cd				
Cd	Cb	Cc	Oc				
Cd	Cb	Cc	Cd				
Ca	Cb	Cd	Cc				
Ca	Cb	Cd	Ha				
Cc	Cb	Cd	Cc				
Cc	Cb	Cd	Ha				
Oc	Cc	Cd	Cb				
Oc	Cc	Cd	Ha				
Cb	Cc	Cd	Cb				
Cb	Cc	Cd	Ha				

Validation of the force field

In order to validate the force field, adsorption energies and isotherms for CO_2 and H_2O are computed and compared to literature data. The adsorption energy is a metric for how well the interaction between the framework atoms and the guest molecules are described. The adsorption isotherm takes into account every influence at once, showing how precise the force field captures the loading dependency.

In Table S6, the results for the adsorption energies of CO_2 are given. The full DFT calculation by Canepa et al.[S12] agrees reasonably well with the full force field model developed in our previous study since the deviation is less than 10% (48.2 $\frac{kJ}{mol}$ to 45.3 $\frac{kJ}{mol}$). The Lennard-Jones based force field model on the other hand underestimates the DFT value by more than 13 $\frac{kJ}{mol}$ indicating that the framework-guest interactions are stronger in reality than described by the Lennard-Jones version. The most likely reason for the deviation is the accuracy loss due to the reparametrization from 4 parameters to 2, in particular for the framework oxygen atoms with the oxygen of the CO_2 molecule. Furthermore, two sets of point charges for the CO_2 molecules were used: one for CO_2-CO_2 interactions and one for CO_2-framework interactions, similar to how water was modeled in Ref. S7.

The adsorption isotherms for CO_2 presented in Figure S7 were measured and calculated at 313 K and pressure up to 1 bar. There is one experimental data by Mason et al.[S8] which serves as the model baseline for the simulated adsorption isotherms of Dzubak et al.,[S9] Sun et al.,[S10] Lin et al.,[S11] and our own. The simulated adsorption isotherms follow the trend of the experimental one measured by Mason et al. yet predict higher uptakes. That was expected since the crystal used in the simulation box is assumed to be perfect with no defects whereas in experiments not all sites are available to the guest molecules.[S9] Our force field is in good agreement with the other DFT-derived force fields due to the reasonable agreement with the adsorption energies and adsorption isotherms.

As for H_2O, the adsorption energies are presented in Table S7. The results based on the Lennard-Jones version of the force field underestimates the DFT value by Canepa et al.[S12]

Table S6: Adsorption energies for CO_2 in Mg-MOF-74 at 300 K.

Force field	Cutoff radius (nm)	Adsorption energy ($\frac{kJ}{mol}$)		
		Monte Carlo	Molecular Dynamics	DFT
Canepa et al.[S12]	—	—	—	48.2
Based on Rudenko et al.[S7]	2.00	45.3 ± 0.1	—	—
This work (rigid, DFT)	1.28	41.9 ± 0.9	42.0 ± 1.0	—
	1.50	42.8 ± 1.8	—	—
UFF	1.28	31.1 ± 0.2	31.9 ± 0.5	—
This work (flexible, DFT)	1.28	—	42.1 ± 1.3	—

and the previously published force field[S7] by less than 5 $\frac{kJ}{mol}$ or 7%, respectively. That means the framework-guest interactions are described sufficiently well. Experimental adsorption isotherms for water reported by Yang et al.[S13] and DeCoste et al.[S14] as well as simulated ones by Lin et al.[S11] and Rudenko et al.[S7] are compared to the fit obtained in this work in Figure S8. There are a lot more experimental isotherms to be found in literature, however, the ones selected here are the maximum and minimum of those. The simulated isotherms by Lin et al. and our previous work follow the trend of the experiments well whereas the former lies outside the range of experiments and the latter lies within. The isotherm based on the force field used int his work does not capture the trend of the experimental isotherms perfectly, as evident by the small step at around 150 pa and by the fact that a saturation loading is reached at around 33 $\frac{mol}{kg}$. Yet, the isotherm is well within the range stretched by the experimental data. Considering the fact that the degrees of freedom have been reduced, the force field is representing the reality accurately enough.

In conclusion, the refitted force field used in this work is not as accurate as the DFT-derived force fields in their full function, but the agreement with literature data for adsorption energies and isotherms is still high. It describes the framework-guest interaction well and is deemed suitable for this study.

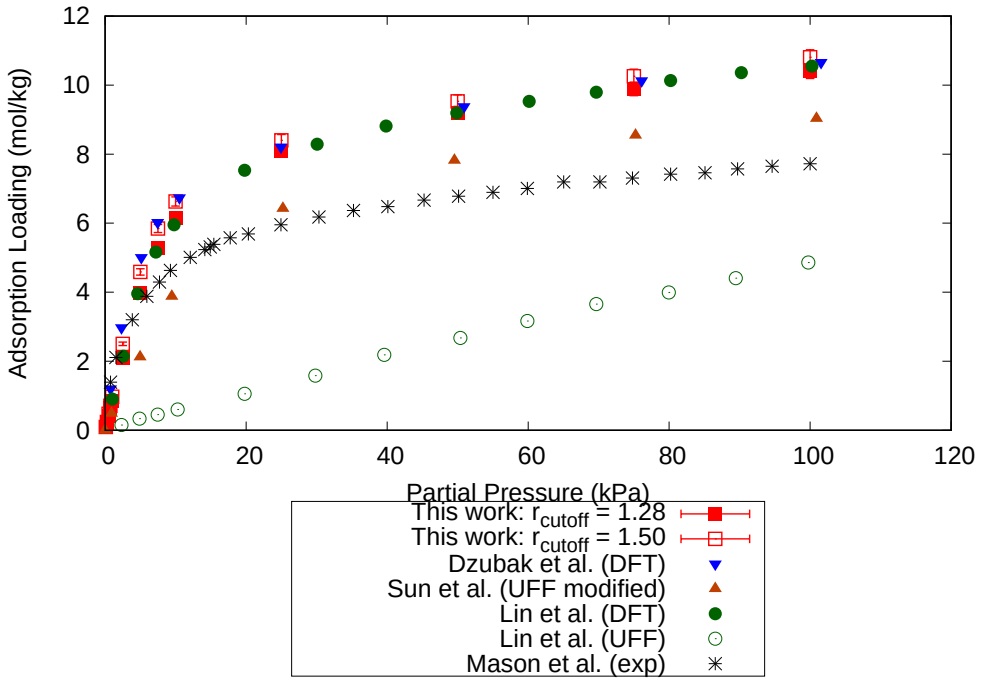

Figure S7: Adsorption isotherm for CO_2 in Mg-MOF-74 at 313 K. Simulation data is taken from Dzubak et al.[S9], Sun et al.[S10], and Lin et al.[S11]. Experiments have been carried out by Mason et al.[S8] Errorbars are too small to be visible.

Influence of cut-off radius r_{cutoff} and simulation length

Due to the refit of the original force field,[S7] it was necessary to verify that the cutoff radius r_{cutoff} for the electrostatic and van der Waals interactions does not influence the outcome of the simulations significantly. Therefore, adsorption isotherms for CO_2 and H_2O in Mg-MOF-74 were calculated with two different r_{cutoff}: 1.28 nm and 1.50 nm. The results can be seen in Figure S7 for CO_2 and Figure S8 for H_2O, respectively. The agreement between the

Table S7: Adsorption energies for H_2O in Mg-MOF-74 at 300 K.

Force field	Cutoff radius (nm)	Adsorption energy ($\frac{kJ}{mol}$)		
		Monte Carlo	Molecular Dynamics	DFT
Canepa et al.[S12]	—	—	—	73.3
Rudenko et al.[S7]	2.00	70.9 ± 0.1	—	—
This work (rigid, DFT)	1.28	68.3 ± 0.2	71.2 ± 1.1	—
	1.50	68.5 ± 0.4	—	—
UFF[S7]	1.28	51.3 ± 3.2	46.3 ± 0.6	—
This work (flexible, DFT)	1.28	—	68.7 ± 1.1	—

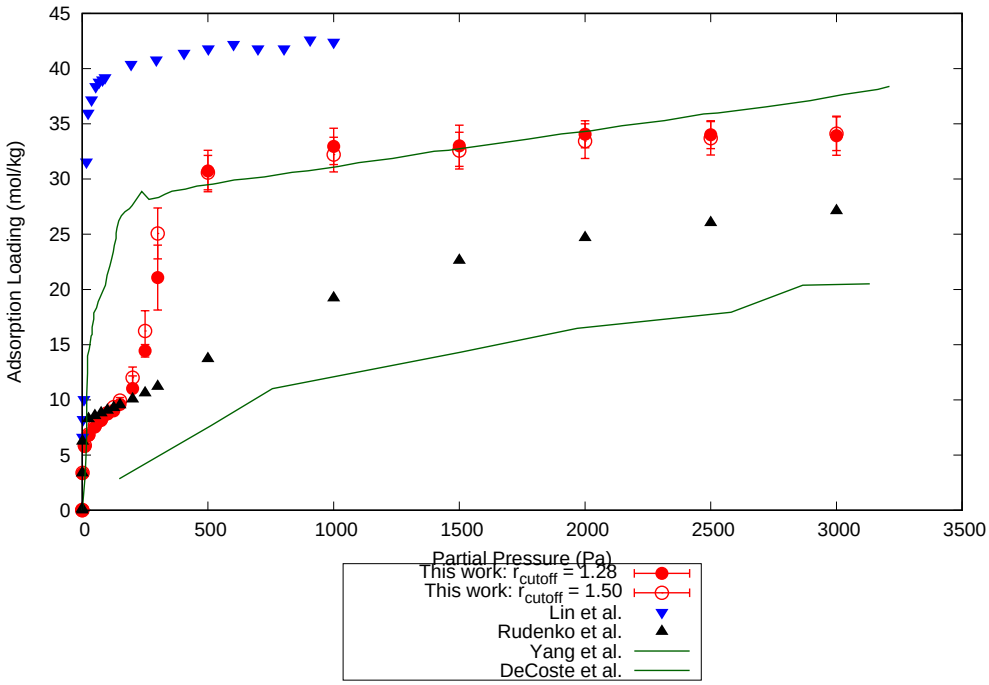

Figure S8: Adsorption isotherm for H_2O in Mg-MOF-74 at 300 K. The data from Yang et al.[S13] and DeCoste et al.[S14] represent the maximum and minimum experimental isotherms for reference, respectively. The data from Rudenko et al.[S7] and Lin et al.[S11] as reference for simulation based isotherms.

refit and the original force field is very good for both guest molecules. If one compares the adsorption energies for the two radii, see Tables S6 and S7, a similar result to the isotherms is found as the energies are within 3% of each other. Ultimately, it can be seen that the greater r_{cutoff} calculates only marginally larger uptake than the smaller one, while the simulation time is increased by up to 50%. As a result, we chose to set r_{cutoff} to 1.28 nm to combine fast simulations with high accuracy.

Table S8: Diffusion coefficients for CO_2 based on simulation length based on the force field used in this work.

Molecules per unit cell	Self-diffusivity in 10^{-8} $(\frac{m^2}{s})$			
	10 ns	30 ns	50 ns	100 ns
1	0.2616 ± 0.0616	0.2504 ± 0.0606	0.2239 ± 0.0205	0.2311 ± 0.0240
2	0.2658 ± 0.0455	0.1844 ± 0.0103	0.2155 ± 0.0063	0.2149 ± 0.0133
10	0.1084 ± 0.0317	0.1040 ± 0.0240	0.0817 ± 0.0050	0.0829 ± 0.0091
20	0.0693 ± 0.0150	0.0646 ± 0.0038	0.0850 ± 0.0113	0.0862 ± 0.0165
36	0.0750 ± 0.0075	0.0638 ± 0.0161	0.0788 ± 0.0163	0.0722 ± 0.0017

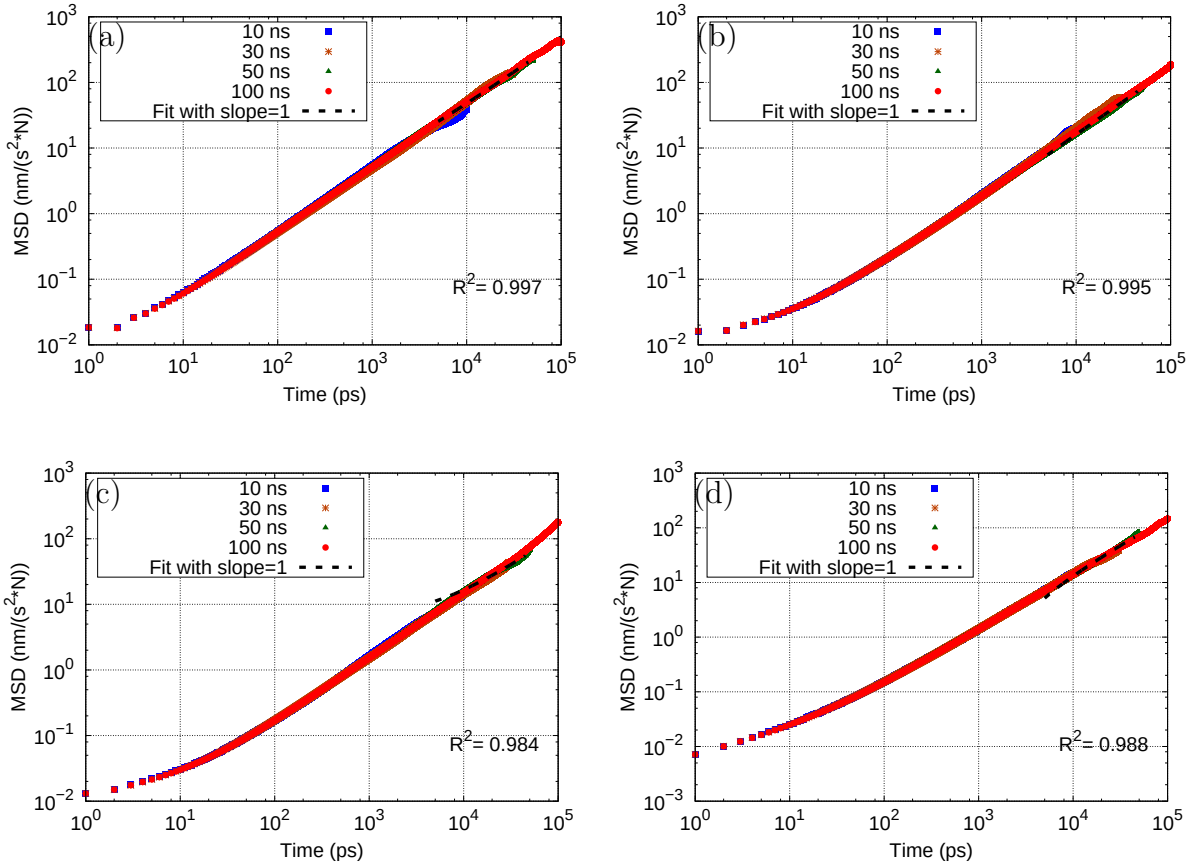

Figure S9: Mean-squared displacement (MSD) for CO_2 in the rigid Mg-MOF-74 as a function of simulation time for 10 ns (blue), 30 ns (brown), 50 ns (green), and 100 ns (red) at 1 (a), 10 (b), 20 (c), and 36 molecules per unit cell (d), respectively.

Next, the influence of the simulation length was investigated. For that, MD simulations with 1, 2, 10, 20, and 36 CO_2 molecules per unit cell at 300 K for 10, 30, 50, and 100 ns were carried out using the rigid framework. The results for the (self-)diffusion coefficients are given in Table S8. It can be seen that the self-diffusivity varies with simulation length regardless of the loading of the simulation box. The highest diffusion coefficients are calculated for 10 ns. Based on the MSD data the diffusion regime has not been reached yet resulting in diffusion coefficients and usually high errors. Similarly, the results for 30 ns almost agree with the ones for 50 ns and 100 ns, however, the corresponding errors for the diffusivity is still quite large whereas the diffusion regime (slope of the fit = 1) is almost reached. Simulating the systems for 50 ns or longer led to small errors and similar diffusion coefficients. The MSD

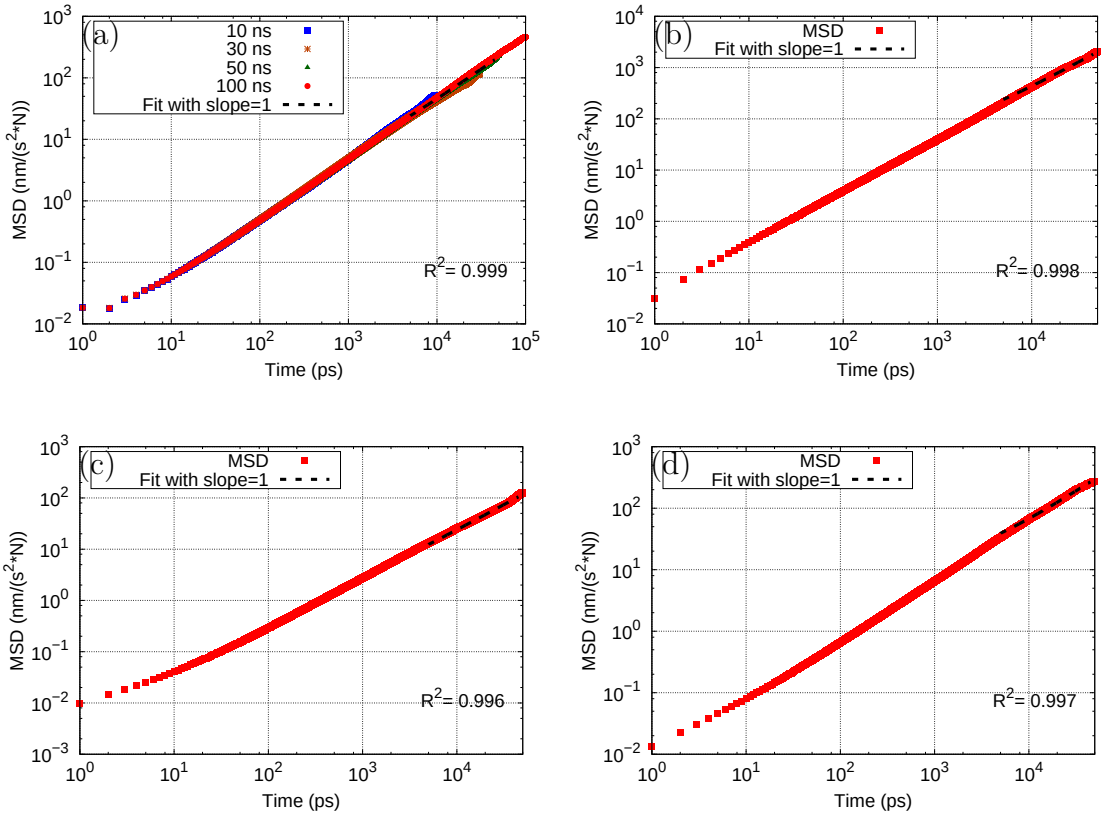

Figure S10: Mean-squared displacement (MSD) for CO_2 in the rigid (a,c) and flexible (b,d) Mg-MOF-74 as a function of simulation time at 2 (a,b) and 36 (c,d) molecules per unit cell, respectively.

plots (Figure S9, S10, and S11) show exemplary for all simulations that the diffusion regime is reached and in a steady state. Thus, we chose the simulation length to be (at least) 50 ns for all of our calculations.

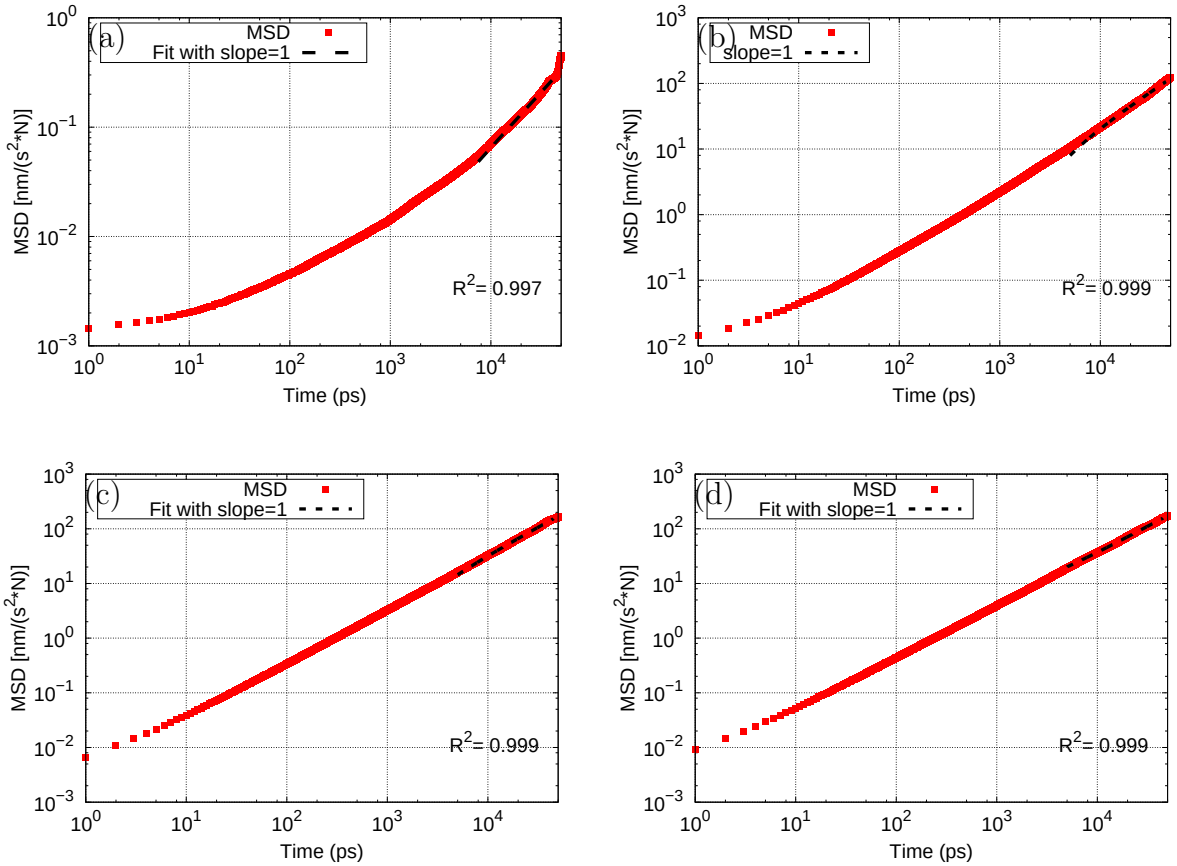

Figure S11: Mean-squared displacement (MSD) for H_2O in the rigid (a,c) and flexible (b,d) Mg-MOF-74 as a function of simulation time at 2 (a,b) and 36 (c,d) molecules per unit cell, respectively.

References

(S1) A. K. Rappe, C. J. Casewit, K. S. Colwell, W. A. Goddard, and W. M. Skiff, *J. Am. Chem. Soc.* **1992**, *114* (*25*), 10024.

(S2) W. L. Jorgensen, J. Chandrasekhar, J. D. Madura, R. W. Impey, and M. L. Klein, *J. Chem. Phys.* **1983**, *79* (*2*), 926.

(S3) D. J. Price and C. L. Brooks, *J. Chem. Phys.* **2004**, *121* (*20*), 10096.

(S4) M. W. Mahoney, W. L. Jorgensen, *J. Chem. Phys.* **2000**, *112*, 8910-8922.

(S5) S. W. Rick, *J. Chem. Phys.* **2004**, *120*, 6085-6093.

(S6) J. J. Potoff and J. I. Siepmann, *AlChE* **2001**, *47*, 1676-1682.

(S7) A. N. Rudenko, S. Bendt, and F. J. Keil, *J. Phys. Chem. C.* **2014**, *118*, 16218-16227.

(S8) J. A. Mason, K. Sumida, Z. R. Herm, R. Krishna, J. R. Long, *Environ. Sci. Technol.* **2011**, *4*, 3030-3040.

(S9) A. L. Dzubak, L.-C. Lin, J. Kim, J. A. Swisher, R. Poloni, S. N. Maximoff, B. Smit, L. Gagliardi, *Nat. Chem.* **2012**, *4*, 810-816.

(S10) W. Sun, L.-C. Lin, X. Peng, B. Smit, *AlChE* **2014**, *60*, 2314-2323.

(S11) L.-C. Lin, K. Lee, L. Gagliardi, J. B. Neaton, B. Smit, *J. Chem. Theory and Comput.* **2014**, *10*, 1477-1488.

(S12) P. Canepa, N. Nijem, Y. J. Chabal, T. Thonhauser, *Phys. Rev. Let.* **2013**, *110*, 026102.

(S13) D.-A. Yang, H.-Y. Cho, J. Kim, S.-T. Yang, W.-S. Ahn, *Energy Environ. Sci.* bf2012, *5*, 6465-6473.

(S14) J. B. DeCoste, G. W. Peterson, B. J. Schindler, K. L. Killops, M .A. Browe, J. J. Mahle, *J. Mat. Chem. A* **2013**, *1*, 11922-11932.